AMERICAN JOURNAL OF INDUSTRIAL MEDICINE 59:301–306 (2016)

The Comparison of High-Resolution Computed Tomography Findings in Asbestosis and Idiopathic Pulmonary Fibrosis

Masanori Akira, MD[1]* and Kenji Morinaga, MD[2]

Background *To determine whether the HRCT findings are useful to differentiate asbestosis from idiopathic pulmonary fibrosis (IPF).*
Methods *We assessed HRCT scans from patients with asbestosis (n = 96) and IPF (n = 65). The frequencies and extent of parenchymal abnormalities and the frequencies of pleural changes were evaluated by consensus of two chest radiologists.*
Results *There was a significant difference between IPF and asbestosis in pleural changes. In addition, there were significant differences between IPF and asbestosis in several parenchymal abnormalities on CT, especially in the less advanced stage of both diseases. On multivariate analysis, HRCT features that distinguished asbestosis from IPF were subpleural lines at a distance of less than 5 mm from the inner chest wall, subpleural dots and parenchymal bands.*
Conclusions *There are significant differences between IPF and asbestosis in the parenchymal and pleural abnormalities on CT.* Am. J. Ind. Med. 59:301–306, 2016.

KEY WORDS: asbestosis; interstitial pulmonary fibrosis; high-resolution CT

INTRODUCTION

Differentiating idiopathic pulmonary fibrosis (IPF) from asbestosis is important because the treatment and prognosis of IPF may differ from those of asbestosis. It is also important because of legal and compensation issues. Differentiating one from the other is often difficult, particularly in patients whose extent of occupational asbestos exposure is unclear. In addition, asbestos-exposed persons potentially are subject to the same spectrum of lung diseases as the general population.

Emphasis has been placed on the presence or absence of pleural plaques or diffuse pleural thickening in discriminating between asbestos-induced pulmonary fibrosis and IPF [Governa et al., 2006; Cox et al., 2014]. However, IPF with pleural plaques can be present. Asbestosis required a heavy exposure to develop, whereas pleural plaques can occur after low or environmental exposure [Hillerdal, 1991].

High-resolution CT (HRCT) is used in the evaluation of asbestos-related lung diseases [Aberle et al., 1988; Al-Jarad et al., 1992; Akira et al., 2003]. The aim of the present study was to identify differences, if any, in HRCT findings between asbestosis and IPF.

METHODS

Patients

Approval for this study was obtained from the institutional clinical research ethics board of each hospital

[1]Department of Radiology, NHO Kinki-Chuo Chest Medical Center, Sakai, Osaka, Japan
[2]Department of the Relief for Asbestos Related Diseases, Environmental Restoration and Conservation Agency, Kawasaki, Japan
*Correspondence to: Masanori Akira, MD, Department of Radiology, NHO Kinki-Chuo Chest Medical Center, 1180 Nagasone-cho, Kita-ku, Sakai, Osaka 591-8555, Japan. E-mail: akira@kch.hosp.go.jp

Accepted 13 January 2016
DOI 10.1002/ajim.22573. Published online 22 February 2016 in Wiley Online Library (wileyonlinelibrary.com).

that participated in the study (Kinki-chuo Chest Medical Center and Osaka Medical Center). The ethical review boards of the institutions that contributed cases did not require the patients' approval or informed consent for the retrospective review of their records and images. Ninety-six consecutive patients with asbestos exposure-induced interstitial fibrosis and 65 consecutive patients with IPF that was seen on HRCT scans between 2002 and 2012 were identified from the hospital radiology database systems of the two referral centers (Table I). The 96 asbestosis patients were diagnosed as asbestosis on the basis of clinical and radiologic criteria, an unequivocal history of substantial asbestos exposure, and time between exposure and onset of symptoms, according to the modified American Thoracic Society criteria for the diagnosis of asbestosis [American Thoracic Society, 2004]. Occupational histories included: textile workers (n = 48), asbestos manufacturing workers (n = 36), asbestos-spraying (n = 7), and shipyard workers (n = 5). In 42 of these 96 patients, asbestosis was also diagnosed on pathologic grounds. Histological diagnosis of asbestosis included diffuse interstitial fibrosis and the presence of two or more asbestos bodies in tissue sections. The 65 patients with IPF met the clinical and histological criteria for the diagnosis as recommended by the ATS/ERS consensus classification of the idiopathic interstitial pneumonias (IIPs) [Travis et al., 2011]. All of these 65 patients were diagnosed histologically as usual interstitial pneumonia (UIP) by two lung pathologists.

Imaging Method and Image Analysis

Chest radiographs were classified according to the International Labour Organization (ILO) classification of the radiographic appearances of the pneumoconiosis [International Labor Office, 2011]. The scoring system was equally applicable to IPF. The HRCT examinations were performed with 1 or 1.5 mm collimation at 15 or 20 mm intervals from the apex of the lung to the diaphragm. The scans were obtained with the patient in the supine position at full inspiration and were reconstructed using a high spatial frequency algorithm. Images were photographed at a window setting appropriate for viewing the lung parenchyma (window level from −650 to −700 Hounsfield units [HU]; window width from 1,200 to 1,500 HU). Each CT examination was viewed simultaneously by two chest radiologists who had no clinical or pathologic informations of the patients. The radiologists evaluated the presence or absence of CT findings, which included the presence of ground glass attenuation, reticular opacities, interlobular septal thickening, traction bronchiectasis, honeycombing, subpleural dots, subpleural lines, parenchymal bands, and mosaic attenuation. The CT findings were interpreted on the basis of the recommendations of the Nomenclature Committee of the Fleischner Society [Hansell et al., 2008]. When subpleural lines were seen, the distance of the subpleural line from the inner chest wall was recorded. The overall extent of parenchymal abnormalities and the extent of ground-glass attenuation and reticular opacities were also assessed. The extent of these abnormalities was determined for six zones (upper, middle, and lower zones in each lung). Each of the six zones was evaluated separately. The six areas of the lung included the upper zones, above the level of the carina; the middle zones, between the level of the carina and the level of the inferior pulmonary veins; and the lower zones, under the level of the inferior pulmonary veins. A score was assigned on the basis of the percentage of lung parenchyma that showed evidence of an abnormality and was estimated to the nearest 10% of parenchymal involvement. Overall percentage of involvement was calculated by averaging the scores of the six lung zones [Akira et al., 2011]. The extent of traction bronchiectasis was evaluated by counting the number of segments that showed evidence of traction bronchiectasis. The presence or absence of pleural changes (pleural plaques and diffuse pleural thickening) were also recorded. The findings from the CT were agreed on by consensus of the two radiologists. We did not use Kusaka et al.'s international classification of HRCT for occupational respiratory diseases [Suganuma et al., 2009], because we wanted to identify differences in HRCT findings between asbestosis and IPF.

TABLE I. Demographic Data and Radiographic Profusion of Study Patients

Characteristics	Asbestosis (n = 96)	Idiopathic pulmonary fibrosis (n = 65)
Sex (M/F)	62/34	42/23
Median age (y; SD)	67 (1.54)	61 (2.29)
Radiograph ILO Profusion		
1	50	18
2	35	33
3	11	14

Statistical Analysis

Data are given as mean ± SD or as patient count and percentage. Wilcoxon's rank sum, Spearman's rank order correlation, and Fisher's exact tests were used for statistical comparisons of HRCT characteristics, as appropriate. Multivariate logistic regression analysis was used to assess the predictive value of the various HRCT findings in

distinguishing asbestosis from IPF. CT features predictive of asbestosis, as opposed to IPF, were identified by means of stepwise forward regression. A stepwise logistic regression model was built using variables with univariate P values of less than 0.20, entering variables at the 0.05 significance level and removing them at the 0.10 level. The Hosmer–Lemeshow test was used for assessing model fit [Hosmer and Lemeshow, 1980].

RESULTS

There was no significant difference in sex among the two groups. Patients with asbestosis were older ($P = 0.001$). Patients with IPF had a higher radiographic profusion compared to patients with asbestosis ($P = 0.007$; Table I). The frequencies and extent of parenchymal abnormalities and the frequencies of pleural changes seen in patients with asbestosis and IPF are shown in Table II. Pleural changes were found in 71 (74%) of 96 patients with asbestosis and in 1 (2%) of 65 patients with IPF. Sixty-nine (72%) patients with asbestosis had pleural plaques, and 25 patients with asbestosis had diffuse pleural thickening. Twenty-five patients with asbestosis had both pleural plaques and pleural thickening. One patient with IPF had diffuse pleural thickening and none with IPF had pleural plaques. There were no significant differences between IPF and asbestosis in the overall extent of parenchymal abnormalities, the extent of ground glass opacities and the extent of reticular opacities; however, there were significant differences in honeycombing and traction bronchiectasis grade. Subpleural dots, subpleural lines, parenchymal bands, and mosaic attenuation were more common in the asbestosis group than in the IPF group.

In profusions 1 and 2, subpleural dots, subpleural lines, parenchymal bands, and mosaic pattern were more common in patients with asbestosis, whereas honeycombing was more common in patients with IPF (Fig. 1). In profusion 3, there were significant differences in overall extent of parenchymal abnormalities, extent of reticular opacities, traction bronchiectasis, subpleural lines, and mosaic attenuation between IPF and asbestosis (Fig. 2); however, there were no significant differences in subpleural dots and honeycombing between the two groups (Table III). Subpleural dots and subpleural lines were found in less severe areas of the pulmonary parenchyma in patients with advanced disease (Fig. 3). The distance of the subpleural lines from the inner chest wall was 2 to 3 mm in all patients with asbestosis, whereas subpleural lines were observed at distances of more than 5 mm from the inner chest wall in patients with IPF (Fig. 4). On multivariate analysis (Table IV), HRCT features that distinguished asbestosis from IPF were subpleural lines at a distance of

TABLE II. HRCT Findings in Patients With Asbestosis and IPF

CT features	Asbestosis group (n = 96)	IPF group (n = 65)	*P*-value
Overall extent	18.9 ± 14.3	20.6 ± 11.1	0.393
GGO extent	5.6 ± 7.1	5.5 ± 3.3	0.950
Reticular opacity extent	14.2 ± 12.9	17.1 ± 10.6	0.118
Traction bronchiectasis grade	4.3 ± 4.6	9.4 ± 4.1	<0.001
Honeycombing	31 (32)	46 (71)	<0.001
Interlobular septal thickening	81 (84)	61 (94)	0.034
Subpleural dots	90 (94)	30 (46)	<0.001
Subpleural lines	82 (85)	16 (25)	<0.001
<5 mm	76 (79)	9 (14)	<0.001
>5 mm	7 (7)	7 (11)	0.311
Parenchymal bands	31 (32)	1 (2)	<0.001
Mosaic attenuation	25 (26)	4 (6)	<0.001
Pleural changes	71 (74)	1 (0)	<0.001
Pleural plaques	69 (72)	0 (0)	<0.001
Diffuse pleural thickening	25 (26)	1 (2)	<0.001

Percentages in parentheses.

FIGURE 1. Subpleural line and subpleural dots seen in mild asbestosis. High-resolution CT scan shows curvilinear line observed at distances of about 2–3 mm from the inner chest wall (arrows). Subpleural dots are also seen (arrowheads). The subpleural lines are created by connection of subpleural dots arranged along the inner chest wall.

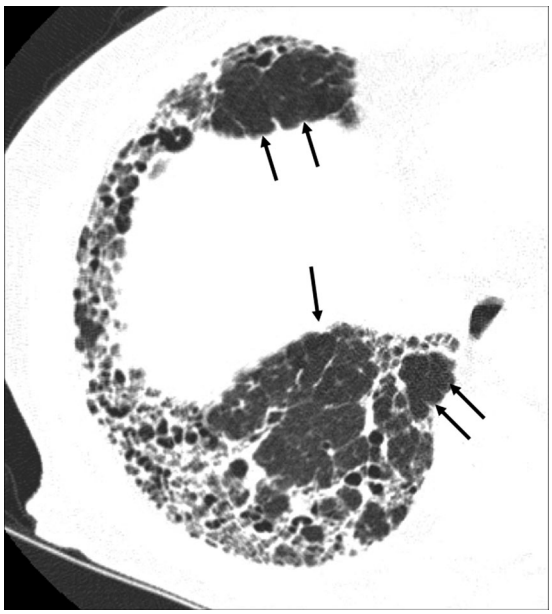

FIGURE 2. Honeycombing seen in advanced IPF. Areas of ground glass attenuation, honeycombing, and traction bronchiectasis are seen in subpleural region of the lung parenchyma. Hyperinflated normal-appearing areas adjacent to the diseased areas are seen (arrows). Note that there are no subpleural dots and subpleural lines.

less than 5 mm from the inner chest wall (odds ratio, 17.68; 95% confidence interval, 7.69–40.65), subpleural dots (odds ratio, 12.09; 95% confidence interval, 3.84–38.02), and parenchymal bands (odds ratio, 12.12; 95% confidence interval, 1.15–128.12).

DISCUSSION

Seventy-four percent of the patients with asbestosis had accompanying pleural thickening. Pleural plaques were found in 72% with asbestosis and were not found in IPF. Pleural plaques are useful for differentiating asbestosis from idiopathic pulmonary fibrosis. Copley et al. [2003] evaluated the HRCT features between asbestosis and IPF and tested the findings in a subset of histopathologically proven cases of UIP and NSIP and found that, after controlling for extent of fibrosis, patients with asbestosis had coarser fibrosis than those with IPF, and that the asbestosis cases involved coarser fibrosis than the NSIP cases but the fibrosis was similar to that in the UIP cases. They concluded that the HRCT pattern of asbestosis closely resembles that of biopsy-proved UIP and differs markedly from that of biopsy-proved NSIP. We previously reported that subpleural dots, subpleural lines, mosaic attenuation, and parenchymal bands were more common in patients with asbestosis, whereas traction bronchiectasis and honeycombing were more common in patients with IPF [Akira et al., 2003].

In the present study, we evaluated the frequency of parenchymal abnormalities in asbestosis and IPF according to the grade of fibrosis. We found that the frequency of parenchymal abnormalities in asbestosis differed according to the grade of fibrosis. In less advanced stage, the frequent HRCT findings of asbestosis included subpleural dots, subpleural lines, and intralobular reticular opacities. Honeycombing and traction bronchiectasis were less frequently found in the patients. Subpleural dots and subpleural lines in the

TABLE III. HRCT Findings in Patients With Asbestosis and IPF

	Profusion ≤ 2			Profusion $= 3$		
CT features	**Asbestosis (n = 85)**	**IPF (n = 51)**	***P*-value**	**Asbestosis (n = 11)**	**IPF (n = 14)**	***P*-value**
Overall extent	17.5 ± 10.5	17.0 ± 8.3	0.769	46.0 ± 14.0	34.0 ± 10.2	0.020
GGO extent	5.8 ± 7.9	4.7 ± 2.9	0.263	7.0 ± 2.8	8.3 ± 3.0	0.287
Reticular opacity extent	12.8 ± 8.4	14.1 ± 7.8	0.354	41.2 ± 11.8	28.2 ± 12.3	0.014
Traction bronchiectasis grade	4.2 ± 4.3	8.3 ± 3.8	<0.001	10.4 ± 3.2	13.2 ± 2.8	0.027
Honeycombing	23 (27)	34 (67)	<0.001	8 (73)	12 (86)	0.623
Interlobular septal thickening	71 (84)	48 (94)	0.107	10 (91)	13 (93)	0.697
Subpleural dots	82 (96)	73 (45)	<0.001	8 (73)	7(50)	0.414
Subpleural lines	75 (88)	15 (29)	<0.001	7 (64)	1 (7)	0.007
<5 mm	69 (81)	9 (18)	<0.001	7 (64)	0 (0)	0.003
>5 mm	6 (7)	6 (12)	0.365	1 (9)	1 (7)	0.697
Parenchymal bands	30 (35)	1 (2)	<0.001	1 (9)	0 (0)	0.440
Mosaic attenuation	20 (24)	3 (6)	0.009	5 (45)	1 (7)	0.039
Consolidated fibrosis	23 (27)	8 (16)	0.144	7 (64)	1 (7)	0.007
Pleural changes	63 (74)	1 (2)	<0.001	8 (73)	0 (0)	<0.001
Pleural plaques	61 (72)	0 (0)	<0.001	8 (73)	0 (0)	<0.001
Diffuse pleural thickening	18 (21)	1 (2)	0.002	7 (64)	0 (0)	0.001

Percentages in parentheses.

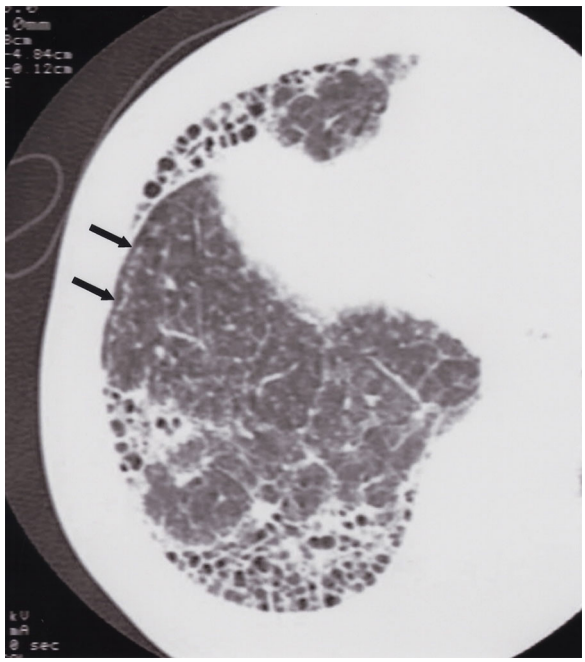

FIGURE 3. Subpleural dotlike lesions and subpleural lines seen in advanced asbestosis. Honeycombing are seen in subpleural region of the lung parenchyma. Subpleural dots forming in line are seen in the subpleural resion of less affected parenchyma (arrows).

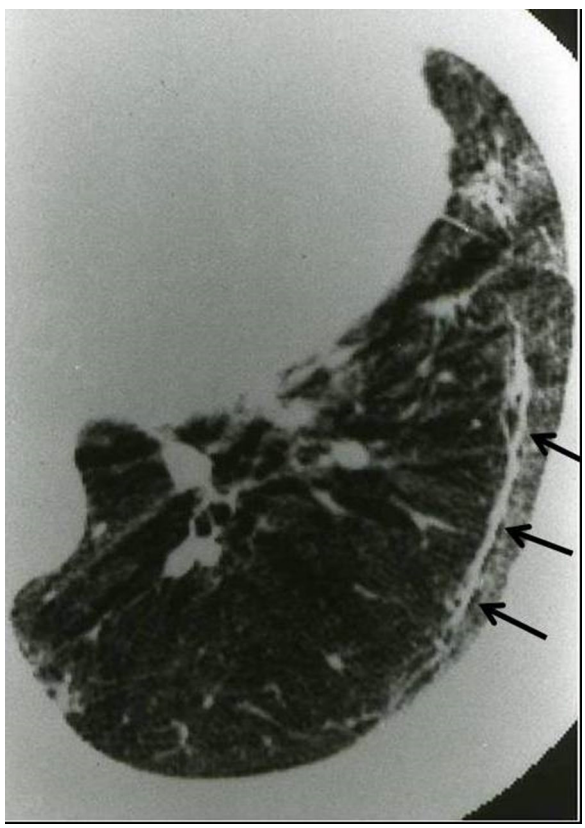

FIGURE 4. Subpleural lines seen in mild IPF. Subpleural lines are seen more than 5 mm from the inner chest wall (arrows).

TABLE IV. Multivariate Logistic Regression Analysis

Parameter	Hazard ratio	95% confidence interval	*P*-value
Subpleural dots	12.09	(3.84, 38.02)	<0.001
Subpleural lines	5.22	(2.14, 12.72)	<0.001
Subpleural lines			
<5 mm	17.68	(7.69, 40.65)	<0.001
>5 mm	0.43	(0.11, 1.75)	0.241
Septal lines	0.24	(0.06, 1.04)	0.057
Parenchymal bands	12.12	(1.15, 128.12)	<0.001
Mosaic pattern	2.82	(0.70, 11.32)	0.145
Honeycombing	0.35	(0.15, 0.86)	0.021

patients with profusions 1 and 2 were more frequent than those in the patients with profusion 3. In advanced asbestosis, subpleural dots and lines may be masked because they are overlaid with intralobular reticular opacities and severe fibrosis. However, subpleural dots and subpleural lines are found in less severe areas of the pulmonary parenchyma in patients with advanced disease. Our study demonstrates that even for higher X-ray profusions it is still possible to detect differences in HRCT findings that may distinguish asbestosis from UIP.

We classified subpleural lines into two categories; <5 mm or ≥5 mm from the inner chest wall. Subpleural lines, in the cases with IPF, were often observed at distances of about 1.5–2 cm from the inner chest wall. The distance of the subpleural lines from the inner chest wall was 2 to 3 mm in patients with asbestosis, which indicates pathologically that the subpleural lines represent peribronchiolar fibrotic thickening combined with flattening and collapse of the alveoli due to fibrosis [Akira, 2008]. The subpleural lines appear to represent connection of subpleural dots arranged along the inner chest wall on the HRCT.

Our study has some limitations. The patients with clinically diagnosed asbestosis group might have both asbestosis and IPF. However, in all our cases with asbestosis, the clinical progression was slow or had stabilized over time, which is compatible with asbestosis. A selection bias may have been introduced into the study by including only patients with biopsy-proved IPF. IPF patients having typical HRCT findings seldom undergo lung biopsy. All CT examinations were performed using HRCT technique and with the patient supine. Because the scans were performed at 15–20 mm intervals, it is also conceivable that small abnormalities and pleural changes may have been missed between CT sections. A study has shown that low-dose (60–100 mA) spiral CT, with reconstruction of contiguous 5 mm thick images is comparable with HRCT at 30 mm intervals in the detection of pleural plaques and parenchymal fibrosis [Remy-Jardin et al., 2004]. Prone scans are useful in evaluating the patients with early stage asbestosis [Chong et al., 2006]; however, in our study prone HRCT scans were not available in all patients with asbestosis and IPF.

In conclusion, comparing the HRCT findings in asbestosis and IPF, there were significant differences between IPF and asbestosis in several CT findings, especially in the less advanced stages of both diseases. The HRCT features that best differentiated asbestosis from IPF were pleural plaques, subpleural lines at distance of less than 5 mm from the inner chest wall, subpleural dots and parenchymal bands that can be found in less severe areas of the pulmonary parenchyma in patients with advanced disease.

AUTHORS' CONTRIBUTIONS

MA has contributed conception and design of the study, acquisition of data, analysis and interpretation of data, and drafting the manuscript. KM has contributed conception and design, acquisition of data, analysis and interpretation of data, and drafting the manuscript.

ACKNOWLEDGMENTS

We thank Drs. Hirotaro Miura, Takumi Kishimoto, and Moka Tamura for their assistance.

FUNDING

This study is partly supported by a grant to the Diffuse Lung Disease Group from the Ministry of Health Labour and Welfare, Japan, and the Grant to the Research Grant for the Respiratory Network, National Hospital Organizational, Japan.

DISCLOSURE (AUTHORS)

The authors report no conflict of interest.

DISCLOSURE BY AJIM EDITOR OF RECORD

Steven Markowitz declares that he has no competing or conflicts of interest in the review and publication decision regarding this article.

REFERENCES

Aberle DR, Gamsu G, Ray CS, Feuerstein IM. 1988. Asbestos-related pleural and parenchymal fibrosis: Detection with high-resolution CT. Radiology 166:729–734.

Akira M. 2008. Imaging of occupational and environmental lung diseases. Clin Chest Med 29:117–131.

Akira M, Yamamoto S, Inoue Y, Sakatani M. 2003. High-resolution CT of asbestosis and idiopathic pulmonary fibrosis. AJR Am J Roentgenol 181:163–169.

Akira M, Inoue Y, Arai T, Okuma T, Kawata Y. 2011. Long-term follow-up high-resolution CT findings in non-specific interstitial pneumonia. Thorax 66:61–65.

Al-Jarad N, Strickland B, Pearson MC, Rubens MB, Rudd RM. 1992. High resolution computed tomographic assessment of asbestosis and cryptogenic fibrosing alveolitis: A comparative study. Thorax 47: 645–650.

American Thoracic Society. 2004. Diagnosis and initial management of nonmalignant diseases related to asbestos. Am J Respir Crit Care Med 170:691–715.

Copley SJ, Wells AU, Sivakumaran P, Rubens MB, Lee YCG, Desai SR, MacDonald SLS, Thompson RI, Colby TV, Nicholson AG, et al. 2003. Asbestosis and idiopathic pulmonary fibrosis: Comparison of thin-section CT features. Radiology 229:731–736.

Cox CW, Rose CS, Lynch DA. 2014. Imaging of occupational lung disease. Radiology 270:681–696.

Chong S, Lee KS, Chung MJ, Han J, Kwon OJ, Kim TS. 2006. Pneumoconiosis: comparison of imaging and pathologic findings. Radiographics 26:59–77.

Governa M, Monica A, Bellis D, Bichisecchi E, Santarelli L. 2006. Diagnosis of asbestos-related pleuropulmonary diseases. Med Lav 97(3):463–474.

Hansell DM, Bankier AA, MacMahon H, McLoud TC, Muller NL, Remy J. 2008. Fleischner Society: Glossary of terms for thoracic imaging. Radiology 246:697–722.

Hillerdal G. 1991. Pleural plaques in the general population. Ann NY Acad Sci 643:430–437.

Hosmer DW, Lemeshow S. 1980. Goodness-of-fit tests for the multiple logistic regression model. Comm Stat Theory Methods 9:1043–1069.

International Labor Office. 2011. Guidelines for the use of the ILO international classification of radiographs of pneumoconiosis. occupational safety and health series no. 22 (Rev. 2011). Geneva: International Labor Office.

Remy-Jardin M, Sobaszek A, Duhamel A, Mastora I, Zanetti C, Remy J. 2004. Asbestos-related pleuroparenchymal diseases: Evaluation with low-dose four-detector row spiral CT. Radiology 233: 182–190.

Suganuma N, Kusaka Y, Hering KG, Vehmas T, Kraus T, Arakawa H, Parker J, Kivisaari L, Letourneux M, Gevenois PA, et al. 2009. Reliability of the proposed international classification of high-resolution computed tomography for occupational and environmental respiratory diseases. J Occup Health 51:210–222.

Travis WD, Costabel U, Hansell DM, King TE, Jr., Lynch DA, Nicholson AG, Ryerson CJ, Ryu JH, Selman M, Wells AU, et al. 2011. An Official ATS/ERS/JRS/ALAT Statement: idiopathic pulmonary fibrosis: Evidence-based guidelines for diagnosis and management. Am J Respir Crit Care Med 183:788–824.